National Research Network S92

Industrial Geometry

http://www.industrial-geometry.at

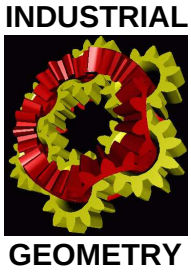

NRN Report No. 108

Texture Enhancing Based on Variational Image Decomposition

Florian Frühauf, Carsten Pontow and Otmar Scherzer

October 2010

FWF
Der Wissenschaftsfonds.

universität wien

Chapter 1
Texture Enhancing Based on Variational Image Decomposition

F. Frühauf, C. Pontow, O. Scherzer

Abstract

In this paper we consider the Augmented Lagrangian Method for image decomposition. We propose a method which decomposes an image into texture, which is characterized to have finite l^1 curvelet coefficients, a cartoon part, which has finite total variation norm, and noise and oscillating patterns, which have finite G-norm. In the second part of the paper we utilize the equivalence of the Augmented Lagrangian Method and the iterative Bregman distance regularization to show that the dual variables can be used for enhancing of specific components. We concentrate on the enhancing feature for the texture and propose two different variants of the Augmented Lagrangian Method for decomposition and enhancing.

Key words: Image decomposition, image enhancement, anisotropic diffusion, texture, curvelets, total variation

1.1 Introduction

The problem of simultaneous reduction of noise and enhancement of important information in image data is an active research area in image analysis. The motivation for this work comes from specifying texture as important image feature. We base

Florian Frühauf
Hauptstrasse 1c/1, 6074 Rinn, Austria

Carsten Pontow
Computational Science Center, University of Vienna, Nordbergstr. 15, 1090 Vienna, Austria

Otmar Scherzer
Radon Institute of Computational and Mathematics, Austrian Academy of Sciences, Altenberger Str. 69, 4040 Linz, Austria and
Computational Science Center, University of Vienna, Nordbergstr. 15, 1090 Vienna, Austria

our work on recently developed variational *image decomposition* models, which separate the image f into independent components.

Given image data f, *variational* decomposition models developed from *variational denoising* methods, which are written in the form

$$\arg\min\{\Phi_0(v_0)+\alpha_1\Phi_1(v_1) : f = v_0+v_1\} . \tag{1.1}$$

Here Φ_0 and Φ_1 are appropriate functionals and $\alpha_1 > 0$ is an appropriate tuning parameter. The paradigm of such a method is the Rudin-Osher-Fatemi (ROF) model [12] which consists in calculating the minimizer of

$$\arg\min\left\{\int_\Omega |v_0|^2+\alpha_1 J(v_1) : f = v_0+v_1\right\}, \tag{1.2}$$

where $J(v_1)$ is the total variation of v_1 on Ω. Thus the ROF model is of the form (1.1) with $\Phi_1 = J$ and with Φ_0 the squared distance of the L^2-norm. Typically, the minimizer $\hat{v}_1$ of the ROF functional reveals a blocky structure and looks like a cartoon image, and this is considered the essential image feature of f. Consequently $\hat{v}_0 := f-\hat{v}_1$ is considered noise.

In the recent years research has been devoted to further extract *fine* structures out of the image f (see [9, 7, 11, 2, 1, 15, 5] to mention but a few). This leads to *exact decomposition* models at several scales:

$$\begin{aligned} &\arg\min \mathscr{D}(v_0,v_1,\ldots,v_n) \text{ with} \\ \mathscr{D}(v_0,v_1,\ldots,v_n) &:= \left\{\Phi_0(v_0)+\sum_{i=1}^n \alpha_i\Phi_i(v_i) : f = \sum_{i=0}^n v_i\right\} . \end{aligned} \tag{1.3}$$

By using $f = \sum_{i=0}^n v_i$ in the functional Φ_0 we obtain the following unconstrained optimization problem:

$$\begin{aligned} &\arg\min \mathscr{R}(v_1,\ldots,v_n) \text{ with} \\ \mathscr{R}(v_1,\ldots,v_n) &:= \left\{\Phi_0\left(f-\sum_{i=1}^n v_i\right)+\sum_{i=1}^n \alpha_i\Phi_i(v_i)\right\} . \end{aligned} \tag{1.4}$$

Here, typically Φ_0 is the L^2-norm, or, after discretization, the Euclidean distance l^2, respectively. Image regularization and decomposition, in general, use sophisticated norms Φ_i, $i = 1,2,\ldots,n$.

For instance, an exact decomposition model with four components (i.e., $n = 3$) has been considered in [2]. There the functionals Φ_i, $i = 1,2,3$ used for decomposition are the total variation semi-norm, the G-norm and the dual of a Besov-space norm, respectively. Y. Meyer [9], who introduced the G-norm to the image analysis community, characterized functions with finite G-norm as *texture*. For instance, oscillating functions have a finite G-norm and are paradigms of texture. However, also noise can have finite G-norm, and thus the G-norm contains oscillating patterns as well as noise. This becomes evident from our compuations where the middle left

image of Figure 1.2, and Figure 1.3, respectively, show oscillating structures from the silhouette of the Zebra and noise.

In our work we investigate an exact decomposition into a cartoon part (using the total variation semi-norm), a texture component (which has a finite norm on a curvelet space) and a noise component (meaning finite E-norm, which has also been considered in [9] and is equivalent to the G-norm). The motivation for this work is to consider curvelet components as texture, because they characterize very well anisotropic structures of different lengths, which are inherent in many images (cf. [8, 3]). At this point we mntion that already in [14] curvelet based functionals have been used, however, there to characterize the cartoon part.

The second part of paper is concerned with texture enhancing based on decomposition models. We consider a two step approach with several alternatives:

1. The first one is the *Augmented Lagrangian Method* (ALM), for finding a decomposition $(\hat{v}_i)_{i=1}^n$, i.e.,

   $$f = \sum_{i=1}^{n} \hat{v}_i \text{ (note that there is no noise component } \hat{v}_0),$$

   which minimizes the functional

   $$(v_1, \ldots, v_n) \to \sum_{i=1}^{n} \alpha_i \Phi_i(v_i) .$$

   In comparison with standard implementations of ALM, we apply alternating direction minimization with respect to specific components. In such a way it is possible to enhance for instance the texture component. Nowadays, ALM is also called iterative Bregman distance regularization [10], and in this modern terminology the algorithm is formulated below, because it makes transparent the enhancing features of the algorithm. To our best knowledge Bregman distance regularization appears first in [4]. As it was shown in [13], Bregman distance regularization with respect to the texture, which we always denote by v_2 in this paper, enhances it with the dual variable. In fact Bregman distance regularization consists of an explicit step backward in time of a generalized diffusion process, which the later is the enhancing procedure.
2. The work of [14] has been picked up by [8] and iterative Bregman regularization has been used to solve for the compressed sensing problem. The focus of our paper is different, however, because we focus on enhancing with respect to texture components. For enhancing we use the dual variable $\zeta_2 = \lim \zeta_2^{(k)}$ of ALM. This provides a texture enhancement strategy:

   $$v_2^{\text{enh}} = v_2 + \tau \zeta_2 , \tag{1.5}$$

   where τ is chosen significantly larger than 1.

The core of the new enhancing procedure is the decomposition model, which is outlined below in detail.

1.2 Image Decomposition Model

In the following we consider a family of image decomposition models. In what follows everything is considered in a discrete setting. The notation and background information can be found in Section 1.5.

Consider a discrete image $f \in X$, the proposed image decomposition method is to calculate a minimizer of

$$\mathbf{J}(v_1, v_2, v_3) = J(v_1) + \alpha_2 C_{\mathbf{a}}(v_2) + \alpha_3 B^*(v_3/\delta)\,, \tag{1.6}$$

subject to the constraint

$$f = \sum_{i=1}^{3} v_i\,. \tag{1.7}$$

Here,

1. $\|\cdot\|_X$ is the Euclidean norm of the intensities of the noise part v_0,
2. $J(v_1)$ is the discrete total variation of v_1 (cf. (1.15)),
3. $C_{\mathbf{a}}(v_2)$ is the weighted curvelet transform (cf. (1.20)),
4. B^* is an approximation of the dual-norm of the Besov space norm $\dot{B}^1_{1,1}$ (cf. (1.19)).

For evaluating the dual of the Besov space norm at v_3/δ, $B^*(v_3/\delta)$, and the curvelet functional $C_{\mathbf{a}}(v_2)$, respectively, we consider v_2 and v_3 as piecewise constant functions on the pixels and assume that they are extended by zero outside of Ω.

Note that in our setting the choice of the parameter α_3 is irrelevant, because B^* only attains the two values zero and infinity. Thus, without loss of generality, α_3 is set to one in the sequel.

For the solution of the constrained minimization problem, we consider *two* variants of ALM, which are both *alternating direction algorithms*. To describe these two methods at once, we introduce a parameter β, which is 0 for the first method (denoted by ALM1) and 1 for the second method (denoted by ALM2).

- Initialize $k = 0$, $v_i^{(0)} = 0$, $i = 1,2,3$, $\zeta^{(0)} = 0$, and consequently, $v_0^{(0)} = f$. Moreover, choose a sequence of positive parameters $(\tau^{(k)})_k$. [1]
- Assign $k \to k+1$. Check for an appropriate stopping criterion.
  - Given $v_i^{(k-1)}$, $i = 0,1,2,3$ define $v_0^{(k-1)} = f - \sum_{i=1}^{3} v_i^{(k-1)}$.
  - Calculate

$$v_3^{(k)} := \operatorname*{arg\,min}_{v_3} \left\{ \frac{\tau^{(k)}}{2} \| f - v_1^{(k-1)} - v_2^{(k-1)} - v_3 \|_X^2 + B^*(v_3/\delta) \right\}. \tag{1.8}$$

  - Calculate

[1] In general one has to assume that $\sum_{k=0}^{\infty} \tau^{(k)} = \infty$, which, of course, is the case if one simply chooses $\tau^{(k)} = \tau > 0$.

$$v_1^{(k)} := \arg\min_{v_1} \left\{ \frac{\tau^{(k)}}{2} \| f - v_1 - v_2^{(k-1)} - v_3^{(k)} \|_X^2 + DJ(v_1, v_1^{(k-1)}) \right\} \quad (1.9)$$

where we use the term

$$DJ(v_1, v_1^{(k-1)}) = J(v_1) - \beta \left(J(v_1^{(k-1)}) + \left(\zeta_1^{(k-1)}, v_1 - v_1^{(k-1)} \right) \right) . \quad (1.10)$$

Here $\zeta_1^{(k-1)}$ denotes an element of the subgradient of J at $v_1^{(k-1)}$. That is, for $\beta = 1$, $DJ(v_1, v_1^{(k-1)})$ is the Bregman distance of the total variation semi-norm and for $\beta = 0$ it is the total variation semi-norm.

– Calculate

$$v_2^{(k)} := \arg\min_{v_2} \left\{ \frac{\tau^{(k)}}{2} \| f - v_1^{(k)} - v_2 - v_3^{(k)} \|_X^2 + \alpha_2 DC_{\mathbf{a}}(v_2, v_2^{(k-1)}) \right\} , \quad (1.11)$$

where

$$DC_{\mathbf{a}}(v_2, v_2^{(k-1)}) = C_{\mathbf{a}}(v_2) - C_{\mathbf{a}}(v_2^{(k-1)}) - \left(\zeta_2^{(k-1)}, v_2 - v_2^{(k-1)} \right) \quad (1.12)$$

denotes the Bregman distance of $C_{\mathbf{a}}$ and $\zeta_2^{(k-1)}$ denotes an element of the subgradient of $C_{\mathbf{a}}$ at $v_2^{(k-1)}$.
This step is identical for both ALM1 and ALM2.

– For ALM2 ($\beta = 1$), motivated from the classical Augmented Lagrangian method, we uses the following update of the dual variable

$$\begin{aligned} \zeta_1^{(k)} &= \zeta_1^{(k-1)} + \tau^{(k)} (f - v_1^{(k)} - v_2^{(k-1)} - v_3^{(k)}) , \\ \zeta_2^{(k)} &= \zeta_2^{(k-1)} + \tau^{(k)} (f - v_1^{(k)} - v_2^{(k)} - v_3^{(k)}) . \end{aligned} \quad (1.13)$$

For ALM1 ($\beta = 0$), we use only the update for $\zeta_2^{(k)}$.

Remark 1. Both algorithms are ad-hoc methods for the solution of the constrained minimization problem. Ad-hoc refers to the fact that in general the subgradient of the sum of three terms is a superset of the sum of the single subgradients. In fact equality only holds if at least one of the subgradients $J(v_1)$ and $C_{\mathbf{a}}(v_2)$ is continuous and $v_3/\delta \in \mathrm{domain}(B^*)$ (see [6]). However, this, a–priori is not guaranteed.

Since each Bregman distance minimization contains an enhancing step (see [13]) by ALM2 only the curvelet components are enhanced, while ALM1 also enhances the total variation component in addition.

Convergence of the ALM algorithm has been proven in a very general setting. In our application, we have a simple situation of a finite dimensional Euclidean space and an l^2 comparison functional

$$(v_1, v_2, v_3) \to \mathscr{E}(v_1, v_2, v_3) = \frac{1}{2} \| f - v_1 - v_2 - v_3 \|_X^2 .$$

Thus the ALM method is convergent in the following sense.

Theorem 1. *Let f be admissible: That is, there exists a triple $(\tilde{v}_1, \tilde{v}_2, \tilde{v}_3)$, which is an element of the domain of* **J**, *such that*

$$\tilde{v}_1 + \tilde{v}_2 + \tilde{v}_3 = f \, .$$

Then the ALM method consisting in minimization of

$$\begin{aligned}(v_1^{(k)}, v_2^{(k)}, v_3^{(k)}) := \underset{(v_1,v_2,v_3)}{\arg\min} \Big\{ \frac{\tau^{(k)}}{2} \| f - v_1 - v_2 - v_3 \|^2 + \\ D\mathbf{J}((v_1, v_2, v_3), (v_1^{(k-1)}, v_2^{(k-1)}, v_3^{(k-1)})) \Big\}\end{aligned} \tag{1.14}$$

satisfies

$$v_1^{(k)} + v_2^{(k)} + v_3^{(k)}) \to f \, .$$

Remark 2. ALM2 is an alternating direction realization of the Augmented Lagrangian Method. To see this, we note that B^* is the characteristic function of the unit sphere with respect to the E-norm. Therefore, the gradient is zero on the domain and $+\infty$ outside. This means that for w in the domain of B^* we have

$$DB^*(w_3, w) = B^*(w_3) \, .$$

Thus in each iteration an alternating direction of the Bregman distance is minimized. Taking into account the equivalence relation of the Bregman distance regularization and ALM, this show that our approach is an alternating direction minimization of the ALM method.

The second difference, resulting from the alternating direction minimization, are two Lagrange parameters $\zeta_i^{(k)}$, i=1,2. The standard ALM only uses one: According to (1.8) and (1.9) we have

$$\begin{aligned}\zeta_1^{(k)} - \zeta_1^{(k-1)} &\in \partial_{v_1} \mathscr{E}(v_1^{(k)}, v_2^{(k-1)}, v_3^{(k)}) \, , \\ \zeta_2^{(k)} - \zeta_2^{(k-1)} &\in \partial_{v_2} \mathscr{E}(v_1^{(k)}, v_2^{(k)}, v_3^{(k)}) \, .\end{aligned}$$

ALM1 leaves out the update with respect to the total variation semi-norm (variable v_1) and enhances only the curvelets component (variable v_2). Therefore ALM1 pronounces the cartoon part more and the according decomposition into texture and noise appears rather intuitive.

1.2.1 Numerical Results

The following image shows some decompositions calculated with the above algorithm. We used as input the noisy Zebra image, Figure 1.1 (right), which was calculated from Figure 1.1 (left) by adding Gaußian random noise of variance 50.

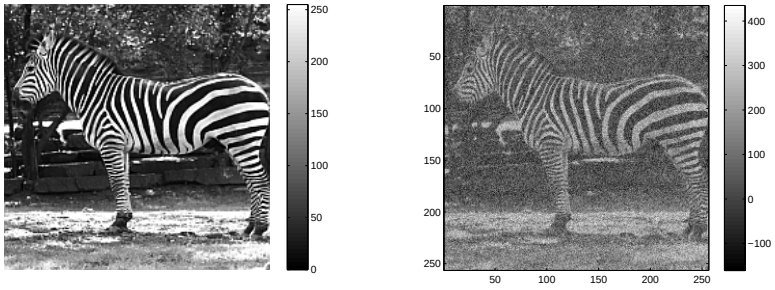

Fig. 1.1 Left: Ideal image. Right: Zebra data, which contains Gaußian random noise of variance 50.

The following images are the output of the ALM1 algorithm after 40 iterations and of the ALM2 algorithm after 20 iterations. In both cases the input image f is decomposed into v_1,v_2, and v_3. We emphasize that after a finite number of iterations the decomposition has only been calculated approximatively, but sufficiently well.

Figure 1.2 shows an approximative decomposition obtained with ALM1, where we used the parameters, $\alpha_2 = 0.6$, $\delta = 58.87$ and the curvelet weights $(a_1, a_2, a_3, a_4, a_5) = (8, 2, 0.02, 0.02, 0.02)$ of $C_{\mathbf{a}}$ (cf. (1.20)). Figure 1.3 shows an approximative decomposition obtained with ALM2, where we used the parameters, $\alpha_2 = 0.15$, $\delta = 58.87$ and the curvelet weights $(a_1, a_2, a_3, a_4, a_5) = (0.5, 0.5, 0.005, 0.005, 0.005)$ of $C_{\mathbf{a}}$ (cf. (1.20).

A comparison of Figure 1.2 and Figure 1.3 shows that ALM1 finds a more distinct separation into components. Especially the cartoon part of ALM2 contains significant textured components.

1.3 Texture Enhancing based on Image Decomposition

For *enhancing* data, a common procedure is by calculating a parabolic diffusion process backward in time. Here, we discuss an enhancing strategy based on dual variables of the ALM method.

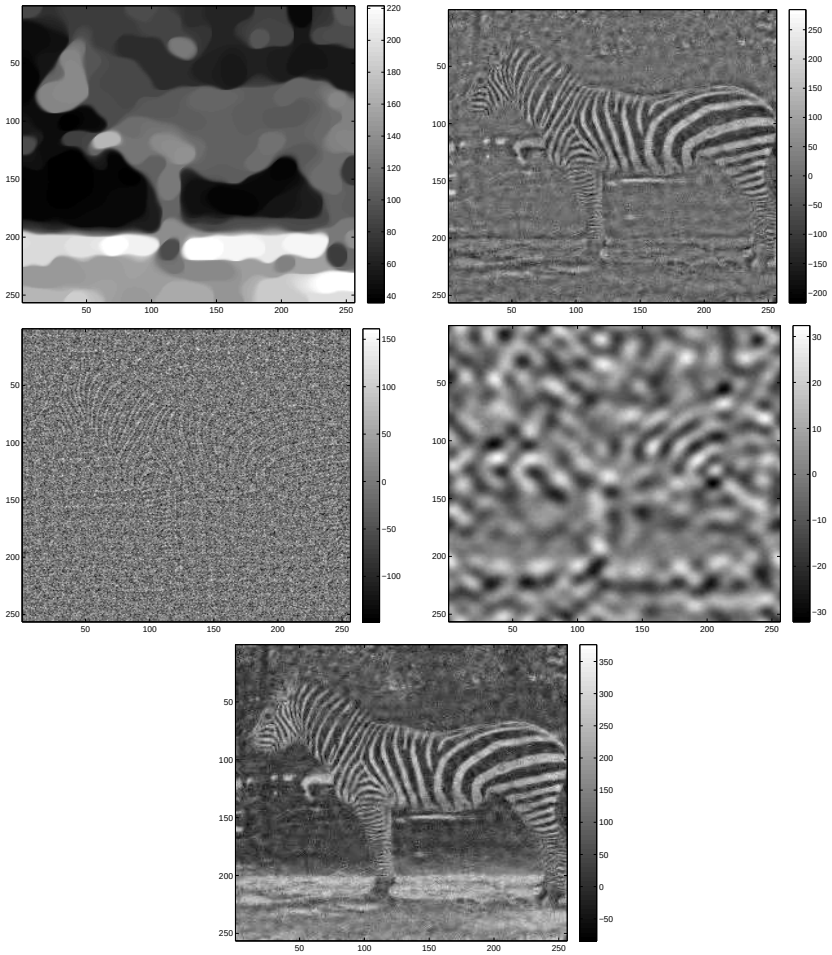

Fig. 1.2 ALM1: Top Left: Cartoon component v_1, Top Right: Texture component v_2, Middle Left: G-norm component v_3. Middle Right:ζ_2. Bottom: Cartoon + Texture: $v_1 + v_2$.

Enhancing with dual variables

The proposed algorithm consists of two steps:

1. Image decomposition: By minimizing the functional **F** defined in (1.6) we calculate three components v_i, $i = 1,2,3$ of $f = v_1 + v_2 + v_3$. We use both ALM1 and ALM2.
2. The second step is by enhancing the texture component. Here, we note that the dual variable $\lim_{k\to\infty} \zeta_2^{(k)} =: \zeta_2 \in \partial C_{\mathbf{a}}(v_2)$ and calculate the enhanced image by

$$v_2^{\text{enh}} = v_2 + \tau\zeta_2$$

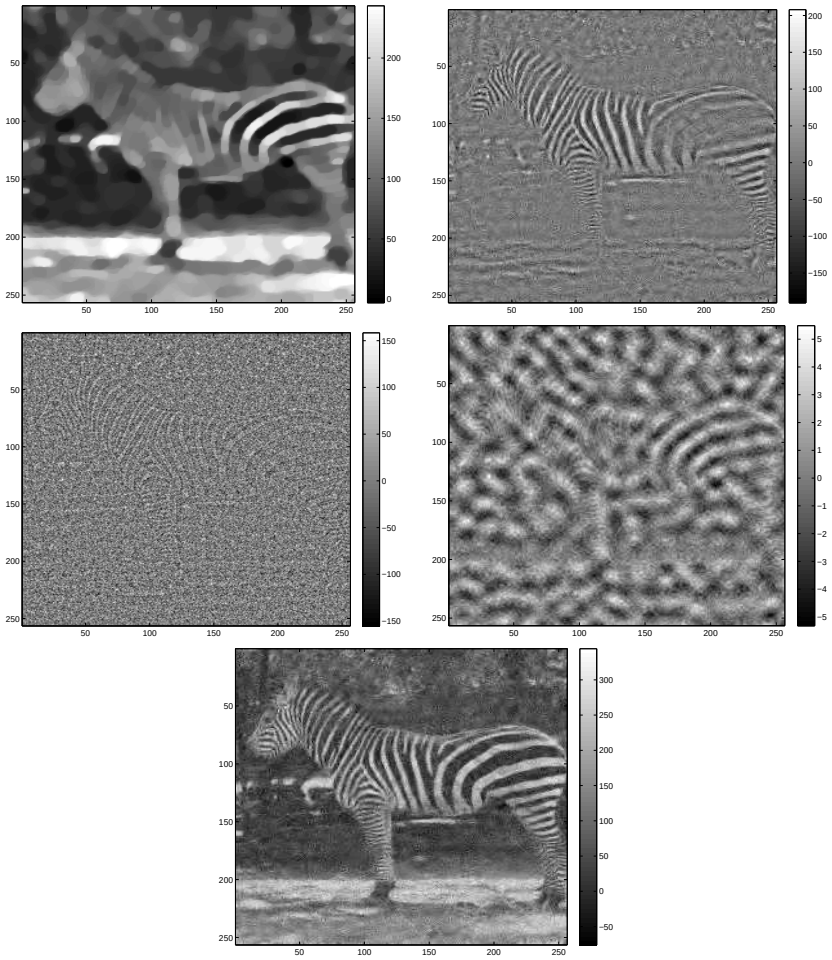

Fig. 1.3 ALM2: Top Left: Cartoon component v_1, Top Right: Texture v_2, Middle Left: G-norm component v_3. Middle Right:ζ_2. Bottom: Cartoon + Texture $v_1 + v_2$.

where τ is significantly larger than 1.

The following images show cartoon enhanced images. In Figure 1.4 we show enhanced texture components by adding 10 times the texture component ζ_2 (dual variable of ALM1 and ALM2, respectively).

Then the image consisting of the sum of the cartoon, the enhanced texture, and the texture component are displayed.

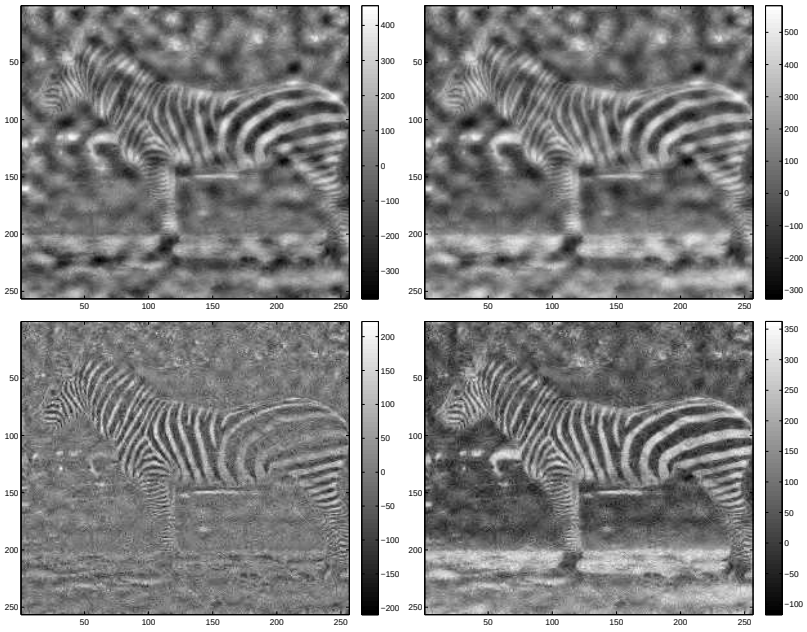

Fig. 1.4 Top Left: ALM2 enhanced texture component of v_2 with $t = 10$. Top Right: ALM2 enhanced image $= v_2^{\text{enh}} + v_1$. Bottom Left: ALM1 enhanced texture component of v_2 with $t = 10$. Bottom Right: ALM1 Enhanced image $=$ enhanced $v_2^{\text{enh}} + v_1$.

1.4 Conclusion

In this paper we have consider two alternating direction variants of the Augmented Lagrangian Method for image decomposition. We have proposed a method which decomposes into texture, which is characterized to have finite l^1 curvelet coefficients, a cartoon part, which has finite total variation norm, and noise and oscillating patterns, which have finite E, G-norm, respectively. So far, the convergence analysis of the two variants is open. In the second part of the paper we have utilized the equivalence of the Augmented Lagrangian Method and the iterative Bregman distance to motivate some methods for texture enhancing. We concentrate on the enhancing feature for the texture and propose two different variants of the Augmented Lagrangian Method for decomposition and enhancing.

1.5 Notations and Some Theoretical Background

Discrete Images:

This paper is devoted to image decomposition and texture enhancing of discrete images.

- A discrete image consists of pixels $\Omega = \{1,\dots,N\}^2$ and intensity values $U := (u_{ij})_{(i,j)\in\Omega}$ associated with the pixels. Therefore every discrete image can be written as a matrix. Wavelets expansion require information on $\mathbb{N}\times\mathbb{N}$. We therefore associate with each image U the extended image $(u_{ij})_{(i,j)\in\mathbb{N}\times\mathbb{N}}$, where $u_{ij} = 0$ for $(i,j)\notin\Omega$.
- $X := \mathbb{R}^{N\times N}$ is the Euclidean space of images. It is associated with the scalar product $(u,v)_X = \sum_{1\le i,j\le N} u_{i,j}v_{i,j}$.
- For $u\in X$ we define the *discrete gradient* ∇u via $(\nabla u)_{i,j} = \left((\nabla u)^1_{i,j},(\nabla u)^2_{i,j}\right)$, where
$$(\nabla u)^1_{i,j} = \begin{cases} u_{i+1,j}-u_{i,j} & \text{if } i<N \\ 0 & \text{otherwise} \end{cases}$$
and
$$(\nabla u)^2_{i,j} = \begin{cases} u_{i,j+1}-u_{i,j} & \text{if } j<N \\ 0 & \text{otherwise.} \end{cases}$$
- The *total variation* of the discrete image u is defined by
$$J(u) = \sum_{1\le i,j\le N} |(\nabla u)_{i,j}| \,. \tag{1.15}$$

Besov Space

In this paper we use the homogeneous Besov spaces $\dot{B}^1_{1,1}$ of functions defined on $\mathbb{R}^2$ and its dual $E := \dot{B}^\infty_{-1,\infty}$. These spaces are defined as follows:

- $\Phi_{j,\mathbf{k}}$ denotes an orthonormal basis of smooth and compactly supported wavelets in $L^2(\mathbb{R}^2)$. The index $j\in\mathbb{Z}$ refers to scale and the index $\mathbf{k}$ refers to position in $\mathbb{R}^2$. That is, each function $u\in L^2(\mathbb{R}^2)$ can be written as
$$u(\mathbf{x}) = \sum_{(j,\mathbf{k})\in\mathbb{Z}^3} c_{j,\mathbf{k}}\Phi_{j,\mathbf{k}}(\mathbf{x}) \text{ for } \mathbf{x}\in\mathbb{R}^2\,, \tag{1.16}$$
where
$$\|u\|_{L^2} = \sum_{(j,\mathbf{k})\in\mathbb{Z}^3} |c_{j,\mathbf{k}}|^2 < \infty.$$
- It can be shown that $\dot{B}^1_{1,1}$ is the space of functions defined on $\mathbb{R}^2$ of the form (1.16) satisfying

$$\sum_{(j,\mathbf{k})\in\mathbb{Z}^3} |c_{j,\mathbf{k}}| < \infty .$$

- The space E denotes the dual space of $\dot{B}^1_{1,1}$. It can be characterized by that the wavelet coefficients of functions in E satisfy

$$\sup_{(j,\mathbf{k})\in\mathbb{Z}^3} |c_{j,\mathbf{k}}| < \infty .$$

  We refer the interested reader for more information on this topic to [9].

Fenchel Duality

- Let $\mathscr{X}$ be a locally convex space (such as $\mathbb{R}^n$ with the Euclidean topology).
- Let $\Phi : \mathscr{X} \to \mathbb{R} \cup \{-\infty, \infty\}$ be a convex, proper, and lower semi-continuous functional. We denote by Φ^* the dual or polar of Φ, i.e.,

$$\Phi^*(v) = \sup_u \left((u,v)_{\mathscr{X}} - \Phi(u) \right) .$$

- For a proper, convex, and lower semi-continuous functional $\Phi : \mathscr{X} \to \mathbb{R}$ and $f \in \mathscr{X}$, the following statements are equivalent (see e.g. [6]):

  1. $\hat{u}$ is a minimizer of the functional

$$u \to \Phi(u) + \frac{1}{2\lambda} \| f - u \|^2_{\mathscr{X}} . \tag{1.17}$$

  2. $\hat{w} := f - \hat{u}$ is a minimizer of the functional

$$w \to \Phi^* \left(\frac{w}{\lambda} \right) + \frac{1}{2\lambda} \| f - w \|^2_{\mathscr{X}} . \tag{1.18}$$

- Let Φ be a semi-norm, then Φ^* is the indicator function of a closed convex set. For instance, let $\Phi(w) = \|w\|_{\dot{B}^1_{1,1}}$ be the norm of the homogeneous Besov space $\dot{B}^1_{1,1}$, then

$$B^*(w/\delta) = \chi_{\delta B_E}(w) = \begin{cases} 0 & \text{if } w \in \delta B_E := \{ w : \|w\|_E \le \delta \} \\ +\infty & \text{otherwise.} \end{cases} \tag{1.19}$$

Curvelets

- Curvelet functions $\psi_{j,\mathbf{k},l}$ form a tight frame of $L^2(\mathbb{R}^2)$. Here j denotes the scale index, l is a index of the angle, and $\mathbf{k}$ is the index of the position. For more background on curvelets we refer to [3] (see also [8]) and references therein.

- Since the curvelet functions are constructed in such a way that they form a tight frame, every function $f \in L^2(\mathbb{R}^2)$ can be expanded in terms of these ansatz functions:
$$u(\mathbf{x}) = \sum_{(j,\mathbf{k},l)\in\mathbb{Z}^4} c_{j,\mathbf{k},l}\,\psi_{j,\mathbf{k},l}(\mathbf{x})$$
and satisfies
$$\|u\|_{L^2}^2 \leq \sum_{(j,\mathbf{k},l)\in\mathbb{Z}^4} |c_{j,\mathbf{k},l}|^2 .$$

- Let $\mathbf{a} = (a_j)$ be a vector of numbers, which are uniformly bounded from below by a positive constant. The (scale) weighted discrete curvelet transform $C_\mathbf{a}$ of a function f is defined by
$$C_\mathbf{a}(u) := \sum_{(j,\mathbf{k},l)\in\mathbb{Z}^4} a_j |c_{j,\mathbf{k},l}| . \tag{1.20}$$
We call the functional $C_\mathbf{a}$ scale-weighted since the value of $C_\mathbf{a}$ is affected differently by the values of a_j.
The subgradient of $C_\mathbf{a}$ at u is the set of all functions with coefficients $u_{j,\mathbf{k},l} \in \operatorname{sgn}(c_{j,\mathbf{k},l})$ for which
$$a_j |u_{j,\mathbf{k},l}| \in l^2 .$$
Here $\operatorname{sgn}(\rho)$ is an element of $[-1,1]$ if $\rho = 0$ and $+1$ if $\rho > 0$ and -1 if $\rho < 0$.

Acknowledgement

The authors express are grateful to Andreas Obereder (Mathconsult Linz) for providing example files on anisotropic diffusion filtering. We also thank Kurt Rabitsch (CSC Vienna) for performing computations at the Vienna Scientific Cluster related. This work has been supported by the Austrian Science Fund (FWF) within the national research networks Industrial Geometry, project 9203-N12, and Photoacoustic Imaging in Biology and Medicine, project S10505-N20.

References

1. J.-F. Aujol, G. Aubert, L. Blanc-Féraud, and A. Chambolle. Image decomposition into a bounded variation component and an oscillating component. *J. Math. Imaging Vision*, 22(1):71–88, 2005.
2. J.-F. Aujol and A. Chambolle. Dual norms and image decomposition models. *Int. J. Comput. Vision*, 63(1):85–104, 2005.
3. E. Candès, L. Demanet, D. Donoho, and L. Ying. Fast discrete curvelet transforms. *Multiscale Model. Simul.*, 5:861–899, 2006.

4. G. A. G. Cidade, C. Anteneodo, N. C. Roberty, and A. J. S. Neto. A generalized approach for atomic force microscopy image restoration with Bregman distances as Tikhonov regularization terms. *Inverse Probl. Sci. Eng.*, 8:1068–2767, 2000.
5. V. Duval, J.-F. Aujol, and L.A. Vese. Mathematical modeling of textures: Application to color image decomposition with a projected gradient algorithm. *J. Math. Imaging Vision*, 37:232–248, 2010.
6. I. Ekeland and R. Temam. *Convex Analysis and Variational Problems*. North-Holland, Amsterdam, 1976.
7. J. Garnett, T. Le, Y. Meyer, and L. Vese. Image decompositions using bounded variation and generalized homogeneous Besov spaces. *Appl. Comput. Harmon. Anal.*, 23(1):25–56, 2007.
8. J. Ma and G. Plonka. Combined curvelet shrinkage and nonlinear anisotropic diffusion. *IEEE Trans. Image Process.*, 16:2198–2206, 2007.
9. Y. Meyer. *Oscillating Patterns in Image Processing and Nonlinear Evolution Equations*, volume 22 of *University Lecture Series*. American Mathematical Society, Providence, RI, 2001.
10. S. Osher, M. Burger, D. Goldfarb, J. Xu, and W. Yin. An iterative regularization method for total variation based image restoration. *Multiscale Model. Simul.*, 4(2):460–489, 2005.
11. S. Osher, A. Solé, and L. Vese. Image decomposition and restoration using total variation minimization and the H^{-1}-norm. *Multiscale Model. Simul.*, 1(3):349–370, 2003.
12. L. I. Rudin, S. Osher, and E. Fatemi. Nonlinear total variation based noise removal algorithms. *Phys. D*, 60(1–4):259–268, 1992.
13. O. Scherzer, M. Grasmair, H. Grossauer, M. Haltmeier, and F. Lenzen. *Variational methods in imaging*, volume 167 of *Applied Mathematical Sciences*. Springer, New York, 2009.
14. J.L. Starck, M. Elad, and D.L. Donoho. Image decomposition via the combination of sparse representations and a variational approach. *IEEE Trans. Image Process.*, 14:1570–1582, 2005.
15. L. Vese and S. Osher. Modeling textures with total variation minimization and oscillating patterns in image processing. *J. Sci. Comput.*, 19(1–3):553–572, 2003. Special issue in honor of the sixtieth birthday of Stanley Osher.